

## ASTER early science outcome and operation status

Hiroji Tsu \*a, Yasushi Yamaguchi \*b, Hiroyuki Fujisada \*c, Anne B. Kahle \*d, Isao Sato \*e,  
Masatane Kato \*f, Hiroshi Watanabe \*f, Masahiko Kudoh \*g, and Moshe Pniel \*h

a Shikoku National Industrial Research Institute, Takamatsu, 761-0395, Japan

b Department of Earth and Planetary Sciences, Nagoya University, Nagoya, 464-8602, Japan

c Remote Sensing Laboratory, Science University of Tokyo, Noda, 278-8510, Japan

d Jet Propulsion Laboratory, MS 183-501, Pasadena, CA 91109, U.S.A.

e Geological Survey of Japan, Tsukuba, 305-8567, Japan

f Earth Remote Sensing Data Analysis Center, Tokyo, 104-0054, Japan

g Japan Resources Observation System Organization, Tokyo, 104-0032, Japan

h Jet Propulsion Laboratory, MS 264-626, Pasadena, CA 91109, U.S.A.

### ABSTRACT

The Advanced Spaceborne Thermal Emission and Reflection Radiometer (ASTER) is a high spatial resolution multi-spectral imaging radiometer, and is onboard the NASA's Terra spacecraft launched on December 18, 1999. It spectrally covers the visible and near-infrared, short-wave-infrared, and thermal infrared regions with 14 spectral bands, and creates high-spatial-resolution (15-90 m) multispectral images of the Earth's surface. The observation performances of the ASTER instrument were evaluated by the early images, e.g. spatial resolution, modulation transfer functions (MTF), signal-to-noise-ratios (SNRs), band-to-band registrations, and so on. It was confirmed that the ASTER instrument generally exceeds the specified observation performance, and the early images exhibit excellent quality even in the preliminary processing level. In the initial check-out phase, ASTER was operationally used for intensive monitoring of volcanic eruptions in Japan, and successfully provided useful information to volcanologists

Keywords: ASTER, Terra, EOS, multispectral imager, instrument characterization, MTF, SNR, volcano monitoring

### 1. INTRODUCTION

The Advanced Spaceborne Thermal Emission and Reflection Radiometer (ASTER) is a high spatial resolution multi-spectral imaging radiometer<sup>1,2,3,4,5,6</sup>. ASTER is onboard the NASA's Terra spacecraft, which was successfully launched aboard Atlas II-AS launch vehicle from Vandenberg Air Force Base in California, U.S.A. at 6:57:39 PM (GMT) on December 18, 1999. Terra is the flagship of the NASA's Earth Observing System (EOS), and carries five observation instruments; ASTER, CERES, MISR, MODIS, and MOPITT<sup>7</sup>. This paper describes the results of ASTER early image evaluation, although more detailed and comprehensive investigation is still being carried out by the ASTER Science Team members. Please note that most of the description, values and images shown in this report are preliminary, and may be changed as a result of further investigation. For more details and updates, please visit the following web site; <http://www.ersdac.or.jp/ASTERProject/ASTERPro.html>

ASTER covers the visible and near-infrared, short-wave-infrared, and thermal infrared regions with 14 spectral bands, and creates high-spatial-resolution (15-90 m) multispectral images of the Earth's surface. ASTER data can be used to help establish a baseline for long-term monitoring of local and regional changes on the Earth's surface, which either lead to, or are in response to, global climate change, e.g., land use, deforestation, desertification, lake and playa water level changes, changes in vegetation communities, glacial movements, and volcanic processes.

The ASTER instrument has three separate optical subsystems (Table 1); the visible and near-infrared radiometer (VNIR), short-wave-infrared radiometer (SWIR), and thermal infrared radiometer (TIR). The VNIR will be especially useful for topographic interpretation because of its along-track stereo coverage with 15 m spatial resolution. The VNIR bands will be also useful in assessing vegetation and iron-oxide minerals in surface soils and rocks. The spectral bandpasses of the SWIR bands were selected mainly for the purpose of surface soil and mineral mapping. Having multispectral TIR data allows for a more accurate determination of the variable spectral emissivity of the land surface, and hence a more accurate determination

of the land surface temperature. Because the data will have wide spectral coverage and relatively high spatial resolution, we will be able to discriminate a variety of surface materials and reduce problems resulting from mixed pixels.

Table 1. ASTER baseline performance requirements

Subsystem	Band No.	Spectral Range ( $\mu\text{m}$ )	Radiometric Resolution	Absolute Accuracy ( $\sigma$ )	Spatial Resolution	Signal Quantization Levels
VNIR	1	0.52 - 0.60	$NE\Delta\rho \leq 0.5 \%$	$\leq \pm 4 \%$	15 m	8 bits
	2	0.63 - 0.69				
	3N, 3B	0.78 - 0.86				
SWIR	4	1.600 - 1.700	$NE\Delta\rho \leq 0.5 \%$	$\leq \pm 4 \%$	30 m	8 bits
	5	2.145 - 2.185	$NE\Delta\rho \leq 1.3 \%$			
	6	2.185 - 2.225	$NE\Delta\rho \leq 1.3 \%$			
	7	2.235 - 2.285	$NE\Delta\rho \leq 1.3 \%$			
	8	2.295 - 2.365	$NE\Delta\rho \leq 1.0 \%$			
	9	2.360 - 2.430	$NE\Delta\rho \leq 1.3 \%$			
TIR	10	8.125 - 8.475	$NE\Delta T \leq 0.3 \text{ K}$	$\leq 3\text{K}(200-240\text{K})$	90 m	12 bits
	11	8.475 - 8.825		$\leq 2\text{K}(240-270\text{K})$		
	12	8.925 - 9.275		$\leq 1\text{K}(270-340\text{K})$		
	13	10.25 - 10.95		$\leq 2\text{K}(340-370\text{K})$		
	14	10.95 - 11.65				

Stereo Base-to-Height Ratio	0.6 (along-track)
Swath Width	60 km
Total Coverage in Cross-Track Direction by Pointing	232 km
MTF at Nyquist Frequency	0.25 (cross-track)
	0.20 (along-track)
Band-to-Band Registration	0.2 pixels (in each telescope)
	0.3 pixels (among different telescopes)
Peak Data Rate	89.2 Mbps
Mass	406 kg
Peak Power	726 W

## 2. INSTRUMENT PERFORMANCE AND IMAGE EVALUATION

The early ASTER images were preliminarily evaluated in order to check observation performance and functionality of the ASTER instrument. We also investigated the early ASTER images from scientific and practical points of view. For instance, the ASTER VNIR image of the San Francisco Bay area (Figure 1) illustrates how the high spatial resolution data can be used to map and monitor local urban environments. We can easily recognize street patterns in the San Francisco downtown areas, various landuse types in the urban areas, characteristic landforms suggesting basement geology, and so on. It is also possible to interpret vortex patterns in the northern bay, which may be caused by inflow of suspended fresh water from rivers.

We confirmed that the measured spatial resolutions in the cross-track direction of all the ASTER subsystems fulfill the specification on observation performance (Table 2). We can expect excellent modulation transfer functions (MTF) from the sharp patterns of the bridges in the Bay Area. Table 3 shows the MTF values for the ASTER VNIR bands, which were actually measured using the VNIR images.



Figure 1. ASTER VNIR band 2 image of San Francisco Bay Area, U.S.A., obtained on March 3, 2000.

Table 2. Spatial resolution (IFOV) in cross-track direction

Subsystem	VNIR (Nadir)	SWIR	TIR
Measured	21.3 $\pm$ 1rad (15.0 m)	43.44 $\pm$ 1rad (30.6 m)	129 $\pm$ 1rad (91 m)
Specified	21.3 $\pm$ 0.4 $\pm$ 1rad (15 $\pm$ 0.28 m)	42.6 $\pm$ 1.2 $\pm$ 1rad (30.0 $\pm$ 0.8 m)	127.8 $\pm$ 3.8 $\pm$ 1rad (90.1 $\pm$ 2.7 m)

Table 3. Modulation transfer functions (MTF) of the ASTER VNIR bands

		Cross Track	Along Track
Specified		$\geq 0.25$	$\geq 0.20$
Measured	Band 1	0.58	0.58
	Band 2	0.46	0.64
	Band 3N	0.49	0.49
	Band 3B	0.52	0.40

Accuracy of the ASTER band-to-band registration is specified as 0.2 pixels for bands in each telescope, and 0.3 pixels for bands among different telescopes. The band-to-band registration is a part of the level-1 data processing, whose algorithm is provided by the ASTER Science Team<sup>8</sup>. Table 4 shows comparison of the level-1 band-to-band registration. Reference bands were selected for each telescope; band 2 for VNIR, band 6 for SWIR, and band 11 for TIR<sup>6</sup>. The numbers in this table are the average values in pixels.

The version 0.0 algorithm is based upon only the pre-launched data, and the version 0.4 algorithm is the version developed for the purpose of the GDS system tests by using the very early actual ASTER data. For the version 0.0, the poor accuracy is mainly due to geolocation errors, most of which were removed in the later versions. The band-to-band registration accuracies have been gradually improved in the versions 0.4 and 0.9 as shown in Table 4. The version 1.0 was delivered to the ASTER GDS on September 22, 2000. We could successfully fulfill the specification in the version 1.0, namely, better than 0.2 pixels for bands in each telescope and better than 0.3 pixels for bands among different telescopes.

Table 4. Band-to-band registration accuracy for ASTER level-1B Data

	Release Date	Band-to-Band Registration Errors		Errors in Elevation Derived from L-1A Stereo Data
		Within Each Telescope	Among Telescopes	
ver.0.0	Pre-launch	About 500-600m (40 pixels in VNIR)		N/A
ver.0.4	May 02, 2000	$\leq 0.5$ pixels	$\leq 3$ pixels	$\leq 1200$ m
ver.0.9 (beta ver.)	Aug. 18, 2000	$\leq 0.5$ pixels	$\leq 1$ pixel	$\leq 5$ m
ver.1.0	Sep. 22, 2000	$\leq 0.2$ pixels	$\leq 0.3$ pixels	$\leq 5$ m

Preliminary evaluations of the signal-to-noise ratios (SNRs) for the VNIR and SWIR data are shown in Table 5. The measured SNRs of the VNIR bands 1 and 2 exceed the specification. The SNR for the band 3 looks slightly lower than the specification. However, these measurements were performed by using the onboard calibration lamps, and the signal level was lower than the defined high level input radiance, which was used to specify the SNRs of the ASTER instrument.

Therefore, we think that the radiometric performance of the VNIR subsystem can meet the specifications, although the more detailed investigation is still under way. For the SWIR subsystem, the SNRs were evaluated by using the onboard calibration lamps as well. The result exhibits very high SNRs for all the SWIR bands, although the radiance used was slightly higher than the defined input radiance to specify the performance. The evaluation results for the other bands were similar, and we concluded that the ASTER VNIR and SWIR bands satisfy the specification.

Table 5. Signal-to-noise ratios (SNRs) of the ASTER VNIR and SWIR bands

Subsystem	VNIR			SWIR					
	1	2	3N	4	5	6	7	8	9
Measured	224.3	200.1	135.8	218	177	181	177	213	212
Specified	>140	>140	>140	>140	>54	>54	>54	>70	>54
Remarks	On-board lamp data, slightly lower than the defined input radiance to specify the performance			On-board lamp data (the minimum values for lamp A), slightly higher than the defined input radiance to specify the performance					

We also evaluated dynamic ranges of the ASTER data. A dynamic range in this particular case is the number of valid digital number (DN) levels of image data. The valid DN levels of actual image data can be determined from the maximum input radiance, quantization levels, and radiance of the imaged target. The maximum input radiance for each ASTER band was specified so as to avoid saturation for targets with very high reflectance, such as clouds and desert, and also to have enough dynamic range for targets with low reflectance, such as vegetation in bands 1 and 2 (Yamaguchi *et al.*, 1998). Quantization levels of the ASTER VNIR and SWIR subsystems are 8 bits, while that of the TIR is 12 bits. Offset DN values were tuned to be always positive and as low as possible. We checked the actual ASTER image data of various different conditions. As a result, we confirmed that there were enough valid DN levels even for a dark target such as dense vegetation, and also found that saturation never occurred even for a bright target such as desert. Therefore, we concluded that the dynamic range of all the ASTER spectral bands is appropriate.

### 3. OPERATION STATUS

Initial activation and function checks of the ASTER instrument were performed in January and February, 2000. The ASTER initial check-out (ICO) phase was roughly divided into two parts; ICO-1 (until March 19, 2000) for the instrument check-out, and ICO-2 (until late August, 2000) for the GDS check-out. During the ICO-1, the first ASTER VNIR image was obtained on January 30, 2000, as a part of the instrument performance check-out. The first SWIR and TIR images were obtained in early February. Preliminary investigation of these image data was carried out accordingly, and we confirmed that the ASTER instrument was functioning well.

On February 28, 2000, target observation using a one-day-schedule (ODS) was started. Target observation means that we can specify an area of interest for ASTER observation by geographical locations on the earth. Before this date, observation was scheduled just by time for the purpose of the instrument check-out. On April 27, 2000, we started observation for the Science Team Data Acquisition Requests (STARs), which include public relations (PR), calibration and validation test sites, and the data acquisition rate became higher than before (Figure 2); the average rate in this period is 200 scenes per day, but 300 to 400 scenes in a normal operation day. On June 22, 2000, data acquisition for the global mapping STARs was started, and the data acquisition rate became even higher; more than 600 scenes per day. The total number of the ASTER scenes obtained has already reached 50,000 scenes, as of August 30, 2000, including all the operation modes (Table 6). It should be noted that in daytime more than 99% of the total scenes were obtained by the full mode. In nighttime S + T (SWIR plus TIR mode mainly for volcano observation) and T-only mode were used almost equally. The reason is that Mt.Usu and Miyakejima volcanoes in Japan erupted in this period, and many scenes were acquired for the purpose of observing these volcanoes in nighttime.

Table 6. The number of ASTER scenes obtained as of August 30, 2000

Day / Night	Daytime			Nighttime		Total
	Full	V-only	V-stereo	S + T	T-only	
Scenes	47,334	263	64	1,350	1,354	50,365

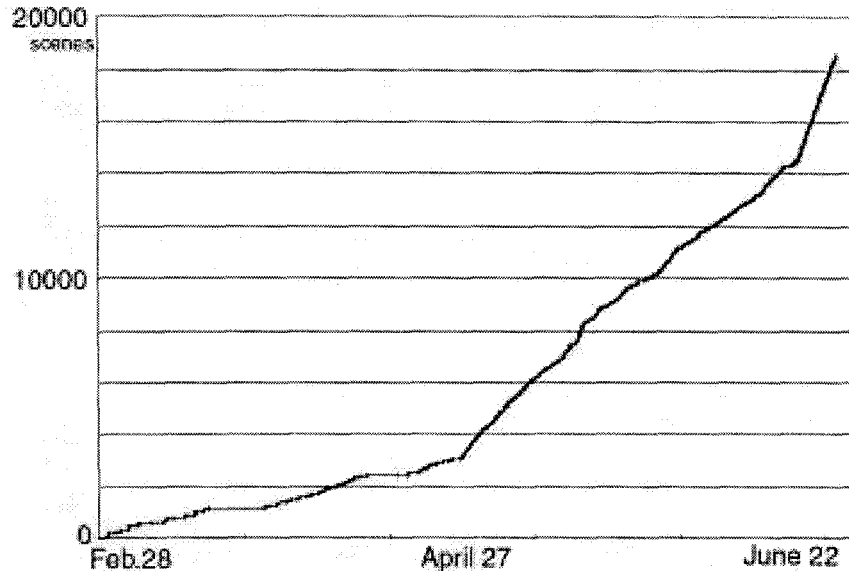


Figure 2. The total number of ASTER scenes obtained as a function of time.

#### 4. INTENSIVE OBSERVATIONS OF ACTIVE VOLCANOES

ASTER is the first spaceborne instrument with high spatial resolution multi-channel thermal infrared imaging for compositional mapping and accurate temperature measurements. In the night of April 14, 2000, ASTER captured the TIR image of Mt.Usu Volcano (Figure 3), Japan, which erupted on March 31. The bright areas in the image indicate high temperature targets including the newly formed craters on March 31 on the northwestern flank of the volcano along with the older lava dome and craters. We also confirmed that the ASTER SWIR images could illustrate distribution of the hot spots in Mt.Usu. This capability is particularly useful to measure high temperature targets that are possibly saturated in TIR imagery. Quantitative evaluation of the ASTER TIR data is still under way, but our preliminary investigations have shown that the TIR subsystem exceeds the specified observation performance. Namely, the radiometric resolution (noise-equivalent-temperature-difference; NEAT) is better than 0.3 K, and the temperature accuracy is better than 1K in the 270 to 340 K region. Considering the spatial resolution (90 m) of the ASTER TIR subsystem, we can expect that the ASTER will be useful for monitoring surface temperature with high radiometric and spatial resolution.

Many earthquakes had been observed since the evening of June 26, 2000, beneath Miyakejima Island, a volcanic island located about 180 km south of Tokyo, Japan. A volcanic eruption occurred in the evening of July 8, 2000, at the summit of Miyakejima Volcano. Since then, volcanic activities still continues even in September, 2000. We scheduled ASTER observations of Miyakejima Volcano, and succeeded in obtaining ASTER data of the volcano on July 1 (daytime and nighttime), July 3 (nighttime), July 8 (nighttime), July 17 (daytime), August 11 (daytime), August 27 (daytime), and September 3 (daytime). Figure 4 is an example of an ASTER VNIR image of Miyakejima Island. We can clearly recognize the wide dark areas of ash fall deposits in the center to eastern parts of the island. These dates do not include failed data acquisitions due to complete cloud cover of the island. All ASTER bands will cover the same 60 km imaging swath with a pointing capability in the cross-track direction to cover  $\pm 116$  km from the nadir, so that any point on the globe is accessible at least once every 16 days with the full spectral coverage with the VNIR, SWIR and TIR. The VNIR subsystem has a larger pointing capability, up to 24 degrees, and thus the swath center is pointable up to  $\pm 318$  km from the nadir. Theoretically, the recurrent pattern for a target on the equator using  $\pm 24$  degrees pointing becomes 2-5-2-7 days (4 days average). Some of the data acquisition for Miyakejima Volcano were performed by the VNIR-only mode in order to shorten a revisit period. Moreover, as shown above we could increase the observation frequency of the Miyakejima Volcano by combining the daytime full mode and nighttime volcano mode (SWIR+TIR). Based upon our actual experience in the ASTER ICO phase, we can conclude that the ASTER pointing capability along with both daytime and nighttime observations were quite useful for intensive observations of an active volcano.

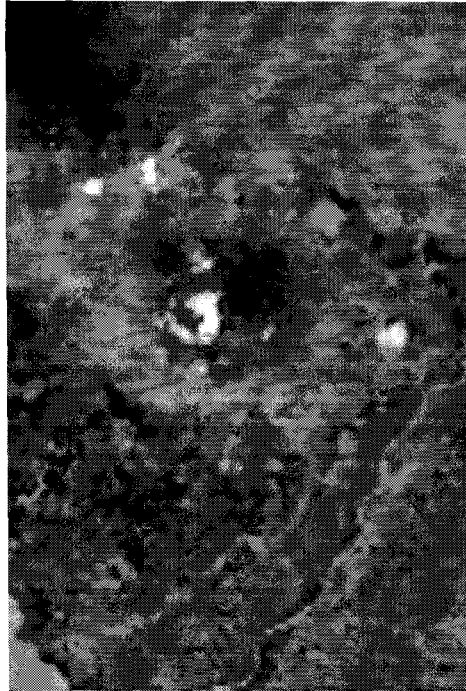


Figure 3. ASTER TIR band 12 image (level 0B1) of Mt.Usu Volcano, Japan, obtained in the night of April 14, 2000. This image covers an area of approximately 7.1 km (E-W) by 10.5 km (N-S) in size. New craters formed by the eruptions in spring, 2000, can be seen in the northwestern corner of the image.

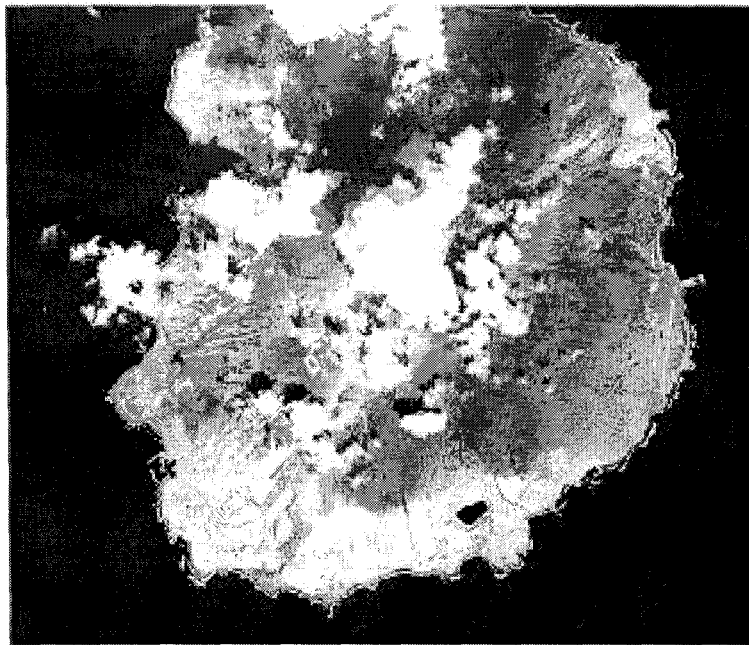


Figure 4. ASTER VNIR band 3 image of Miyakejima Volcano, Japan, obtained in daytime of August 29, 2000. Please note the wide dark areas of ash fall deposits.

## 7. CONCLUSION

The ASTER instrument is functioning well, and its observation performance is exceeding not only the specification but also our expectation. The preliminary investigation results of the ASTER early images exhibit excellent image qualities, although more detailed and comprehensive investigation and evaluation are still under way. We expect that the ASTER data distribution to public will be started soon, and anticipate that various scientific findings will be obtained by using the ASTER data.

## 8. ACKNOWLEDGMENTS

The authors wish to thank the ASTER Science Team members and the ASTER Sensor Committee members for their helpful discussions. The authors are also grateful to many people at NASA, JAROS, ERSDAC, and the contractors for their help in the ASTER Program and for providing valuable information.

## 9. REFERENCES

1. Yamaguchi, Y., H. Tsu and H. Fujisada, "Scientific Basis of ASTER Instrument Design," *Proc. SPIE*, **1939**, pp.150-160, 1993.
2. Yamaguchi, Y., A.B. Kahle, H. Tsu, T. Kawakami, and M. Pniel, "Overview of Advanced Spaceborne Thermal Emission and Reflection Radiometer (ASTER)," *IEEE Trans. Geosci. Remote Sens.*, **36**, pp.1062-1071, 1998.
3. Yamaguchi, Y., H. Fujisada, M. Kudoh, T. Kawakami, H. Tsu, A.B. Kahle, and M. Pniel, "ASTER Instrument Characterization and Operation Scenario," *Advances in Space Research*, **23**, pp.1415-1424, 1999.
4. Fujisada, H., "Overview of ASTER Instrument on EOS-AM1 Platform," *Proc. SPIE*, **2268**, 14-36, 1994.
5. Fujisada, H., "Design and Performance of ASTER Instrument," *Proc. SPIE*, **2583**, pp.16-25, 1995.
6. Fujisada, H., F. Sakuma, A. Ono, and M. Kudoh, "Design and Preflight Performance of ASTER Instrument Protoflight Model," *IEEE Trans. Geosci. Remote Sens.*, **36**, pp.1152-1160, 1998.
7. Kaufman, Y.J., D.D. Herring, K.J. Ranson, and G.J. Gollatz, "Earth Observing System AM1 Mission to Earth," *IEEE Trans. Geosci. Remote Sens.*, **36**, pp.1045-1055, 1998.
8. Fujisada, H., "ASTER Level-1 Data Processing Algorithm," *IEEE Trans. Geosci. Remote Sens.*, **36**, pp.1101-1112, 1998.